arXiv:2504.17490v1 [cs.LG] 24 Apr 2025

Plasticine: Accelerating Research in Plasticity-Motivated Deep Reinforcement Learning

Mingqi Yuan[1*] MINGQI.YUAN@CONNECT.POLYU.HK
Qi Wang[23*] QIWANG067@SJTU.EDU.CN
Guozheng Ma[4*] GUOZHENG001@E.NTU.EDU.SG
Bo Li[1] COMP-BO.LI@POLYU.EDU.HK
Xin Jin[3†] JINXIN@EITECH.EDU.CN
Yunbo Wang[2] YUNBOW@SJTU.EDU.CN
Tao Yu[5] TAO@LIMXDYNAMICS.COM
Xiaokang Yang[2] XKYANG@SJTU.EDU.CN
Wenjun Zeng[3] WZENG-VP@EITECH.EDU.CN
Dacheng Tao[4] DACHENG.TAO@NTU.EDU.SG

[1] *Department of Computing, The Hong Kong Polytechnic University, China*
[2] *MoE Key Lab of Artificial Intelligence, AI Institute, Shanghai Jiao Tong University, China*
[3] *Ningbo Institute of Digital Twin, Eastern Institute of Technology, Ningbo, China*
[4] *College of Computing and Data Science, Nanyang Technological University, Singapore*
[5] *LimX Dynamics, Shenzhen, China*

Abstract

Developing lifelong learning agents is crucial for artificial general intelligence. However, deep reinforcement learning (RL) systems often suffer from plasticity loss, where neural networks gradually lose their ability to adapt during training. Despite its significance, this field lacks unified benchmarks and evaluation protocols. We introduce Plasticine, the first open-source framework for benchmarking plasticity optimization in deep RL. Plasticine provides single-file implementations of over 13 mitigation methods, 10 evaluation metrics, and learning scenarios with increasing non-stationarity levels from standard to open-ended environments. This framework enables researchers to systematically quantify plasticity loss, evaluate mitigation strategies, and analyze plasticity dynamics across different contexts. Our documentation, examples, and source code are available at `https://github.com/RLE-Foundation/Plasticine`.

Keywords: Deep RL, Plasticity, Lifelong Learning, Single-file Implementation

1 Introduction

Developing agents that never stop learning and evolving in dynamic real-world environments represents a critical frontier for advancing artificial intelligence and a fundamental prerequisite for truly developable systems (Abel et al., 2023). Reinforcement learning (RL), with its inherent properties of learning from experience, continual online improvement, and iterative strategic exploration, emerges as the ideal framework for pursuing this objective (Silver and Sutton, 2025). Despite its promise, recent research has increasingly revealed a critical limitation: plasticity loss, a phenomenon in which neural networks in RL agents gradually

∗. Equal contribution.
†. Corresponding author.

©2025 Mingqi Yuan, Qi Wang, Guozheng Ma, Bo Li, Xin Jin, Yunbo Wang, Xiaokang Yang, and Wenjun Zeng.
License: CC-BY 4.0, see `https://creativecommons.org/licenses/by/4.0/`.

lose their ability to adapt and incorporate new information as training progresses (Dohare et al., 2024; Klein et al., 2024), thus significantly impeding the development of truly lifelong learning agents (Lyle and Pascanu, 2024).

This phenomenon emerges specifically when switching from classical tabular RL methods to deep neural architectures (Klein et al., 2024), which explains why it has only recently become a priority in the research community. Additionally, while related to the stability-plasticity trade-off studied in continual (un)supervised learning scenarios, plasticity loss presents a more acute challenge for RL systems due to the pronounced non-stationarity in both data distributions and learning objectives, combined with the bootstrapping mechanisms inherent to RL algorithms (Nikishin et al., 2022). Furthermore, compared to preventing catastrophic forgetting, maintaining plasticity is considerably more critical for developing truly lifelong learnable agents (Abel et al., 2023).

Despite the clear importance of mitigating plasticity loss in deep RL, this field lacks unified methodological frameworks and evaluation protocols. This lack of established benchmarks significantly hampers fair comparisons, methodological consistency, and precise problem formulation. Numerous fundamental questions remain inadequately addressed in current research: • How can we reliably measure and quantify plasticity loss through empirical means? • To what degree do existing mitigation approaches effectively resolve this issue? • In what ways does plasticity loss vary across different task domains and learning scenarios? In response to these challenges, we introduce Plasticine, the first open-source framework for benchmarking plasticity research in deep RL, which currently provides high-quality single-file implementations for 13+ methods, 10+ evaluation metrics, and 3+ learning scenarios.

2 Architecture of Plasticine

Figure 1 illustrates the overall architecture of the *Plasticine* framework, which contains four core parts: **Methods**, **Metrics**, **Environments**, and **Benchmark**. To maximize the convenience for researchers, we adopt the **"single-file"** implementation style that has been widely recognized by the RL community (Huang et al., 2022; Tarasov et al., 2023). More specifically, we put all implementation details of a plasticity loss mitigation method into a single file, including the method logic, hyperparameter configuration, backbone RL algorithm, training environment, and model evaluation. This ensures no intervention exists between different code files and allows researchers to focus on a specific method without worrying about handling special cases while minimizing the workload when developing new methods. In the following content, we introduce the detailed design insights.

2.1 Plasticity Loss Mitigation Methods

Plasticity loss occurs when neural networks gradually develop optimization pathologies during non-stationary RL training processes, causing them to lose their inherent learnability (Nikishin, 2024). Therefore, targeted improvements in various aspects of neural network design have the potential to mitigate plasticity loss. In this benchmark, we have categorized existing mitigation methods based on their primary focus and implemented representative methods for evaluation. The details of each method can be found in Appendix C.

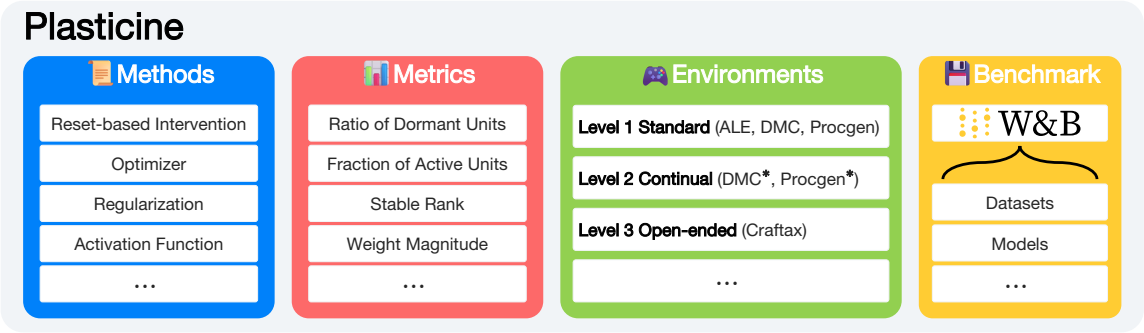

Figure 1: Overview of the Plasticine framework. It consists of 4 core parts: The **Methods** part provides high-quality and single-file implementations of diverse plasticity loss mitigation methods. The **Metrics** part provides comprehensive evaluation metrics to reflect the plasticity variation during training. The **Environments** part provides environmental configurations for different levels of continual RL scenarios, where $*$ denotes a variant designed for the continual scenario. Finally, the **Benchmark** part provides reusable datasets and models for facilitating corresponding research, which is constructed based on **Weights & Biases**.

1. **Reset-based Interventions**: Re-initializing portions of the network represents the most direct approach to regain plasticity (Nikishin et al., 2022), whether through manually selecting specific layers or automatically identifying neurons experiencing severe performance plateaus (Sokar et al., 2023; Galashov et al., 2024).
2. **Normalization**: Normalization techniques, exemplified by Layer Norm, have been shown to be highly effective in mitigating plasticity loss (Nauman et al., 2024). Building on this, more advanced normalization approaches have emerged targeting plastic training, including NaP (Lyle et al., 2024a) and hyperspherical norm (Lee et al., 2025).
3. **Regularization**: Constraining parameter norms or feature rank effectively prevents unbounded growth of weight/feature norms and avoids representation collapse, factors considered highly correlated with plasticity (Kumar et al., 2023; Lyle et al., 2022).
4. **Activation Function**: Alternative activation functions beyond standard ReLU significantly impact neuron activity patterns, helping prevent dead neurons and maintain network capacity throughout non-stationary training (Park et al., 2025).
5. **Optimizer**: Specialized optimization approaches like SAM (Lee et al., 2023) and Fast TRAC (Muppidi et al., 2024) help navigate complex loss landscapes during non-stationary training, thereby maintaining plasticity.

2.2 Comprehensive Evaluation Metrics

Accurately quantifying neural network plasticity remains an open research question (Lyle et al., 2024b). Current methodologies typically involve monitoring multiple plasticity-related indicators from various perspectives and analyzing them holistically (Lee et al., 2024; Ceron et al., 2023). Our benchmark incorporates key metrics directly into the training pipeline, enabling systematic comparison of plasticity dynamics across different approaches. These metrics include the ratio of dormant to active neurons, which indicates possible neuronal pathologies (Sokar et al., 2023; Ma et al., 2024); multiple feature rank measurements

(such as Stable Rank and Effective Rank) that track representation capacity and potential collapse (Lyle et al., 2022); and weight/gradient norm calculations that capture problems such as growth of unbounded parameters and vanishing gradients. This multidimensional evaluation framework helps researchers pinpoint which specific aspects of neural network behavior are most significantly influenced by different plasticity optimization methods.

2.3 Diverse Evaluation Scenarios: Towards Real Lifelong RL

Plasticity loss represents a critical barrier to achieving truly lifelong RL applications, with its severity increasing proportionally to environmental non-stationarity. To comprehensively evaluate both the magnitude of plasticity loss and the effectiveness of mitigation methods, we provide a progressive framework of increasingly non-stationary task scenarios, enabling systematic analysis of how plasticity dynamics evolve across complexity thresholds and quantifying the preservation of learning capabilities as environmental demands intensify.

2.3.1 Level 1: Standard Online RL

Standard online RL naturally exhibits non-stationarity as policies evolve and through bootstrapping processes. In these environments, agents must maintain plasticity throughout training to achieve optimal performance instead of stuck at suboptimal levels. This setting offers a foundation for measuring plasticity during natural distribution shifts in policy optimization without adding explicit task changes. Our baseline evaluation includes popular benchmarks (ALE, Procgen, DMC) that span diverse scenarios with both state-based and vision-based tasks across discrete and continuous action spaces.

2.3.2 Level 2: Continual RL

Continual RL scenarios create more challenging plasticity demands by introducing explicit distribution shifts beyond those naturally occurring in standard RL. We implement two types of scenarios: one where visual features or dynamics models change within the same task, and another requiring adaptation between entirely different tasks. These environments test an agent's ability to maintain plasticity across both sudden task switches and gradual dynamics changes, positioning them between standard and open-ended learning contexts. With clearly defined non-stationarity boundaries, we can directly observe how models behave before and after distribution shifts, gaining valuable insights into plasticity degradation patterns across different task distributions.

2.3.3 Level 3: Open-Ended RL

Open-ended RL presents the highest level of non-stationarity challenge, closely matching real-world lifelong learning needs. We use Craftax (Matthews et al., 2024) as our evaluation environment, which features complex procedural generation without clear task boundaries. Unlike our previous scenarios with structured transitions, Craftax offers an expansive action space with long-horizon dependencies, hierarchical task structures, and continuous novelty. These environments test the frontier of plasticity maintenance, measuring whether agents can preserve learning abilities while navigating constantly evolving challenges, a key requirement for truly lifelong learning systems.

Appendix A. Supplementary Materials

We provide comprehensive supplementary materials to support the **Plasticine** framework:

- Appendix B lists the code file structure of the whole project;
- Appendix C provides the workflow and implementation details of all the implemented methods for plasticity loss mitigation;
- Appendix D introduces the included backbone RL algorithms;
- Appendix E introduces the implementation details of the training environments for the three-level learning scenarios;
- Appendix F provides formally mathematical definitions of the plasticity-related metrics;
- Appendix G provides experimental configurations and results.

Appendix B. Project Structure

```
Plasticine/
├── plasticine/
│   ├── standard/ (Code for the standard RL scenario)
│   │   ├── pqn_atari_vanila.py
│   │   ├── pqn_atari_ln.py (PQN+Atari+Layer Normalization)
│   │   ├── ...
│   │   ├── ppo_procgen_vanilla.py
│   │   ├── ppo_procgen_ca.py (PPO+Procgen+CReLU Activation)
│   │   ├── ...
│   │   ├── td3_dmc_vanilla.py
│   │   ├── td3_dmc_snp.py (TD3+DMC+Shrink & Perturb)
│   │   └── ...
│   ├── continual/ (Code for the continual RL scenario)
│   │   ├── ppo_procgen_vanilla.py
│   │   ├── ppo_procgen_dff.py (PPO+Continual-Procgen+Deep Fourier Features)
│   │   ├── ...
│   │   ├── td3_dmc_vanilla.py
│   │   ├── td3_dmc_trac.py (TD3+Continual-DMC+TRAC Optimizer)
│   │   └── ...
│   └── open/ (Code for the open-ended RL scenario)
│       ├── ppo_craftax_vanilla.py
│       ├── ppo_craftax_redo.py (PPO+Craftax+ReDo)
│       └── ...
├── requirements/ (Dependencies for environments)
│   ├── requirements-prcogen.txt
│   ├── requirements-craftax.txt
│   └── ...
├── scripts/ (Training scripts)
├── experimental/ (Experimental code files)
└── assets/ (Miscellaneous files)
```

Appendix C. Details of Implemented Plasticity Optimization Methods

C.1 Reset-based Intervention

C.1.1 Shrink and Perturb

Shrink and perturb (SnP) (Ash and Adams, 2020) periodically scales the magnitude of all weights in the network by a factor and then adds a small amount of noise. For a set of parameters Θ, SnP adjusts them by

$$\Theta = \alpha\Theta_{\text{current}} + \beta\Theta_{\text{init}}, \tag{1}$$

where $\alpha = 1 - \beta$ and Θ_{init} is sampled from the initialization distribution of parameters.

We provide two options for the SnP operation: The user can choose to invoke it at specific intervals or after each gradient descent step (Soft SnP).

C.1.2 Plasticity Injection

Plasticity injection (PI) (Nikishin et al., 2023) replaces the final layer of a network with a new function that is a sum of the final layer's output and the output of a newly initialized layer subtracted by itself. The gradient is then blocked in both the original layer and the subtracted new layer. In practice, the PI operation is only applied to the final layers of the network.

C.1.3 ReDo

This technique resets individual neurons within the network based on a dormancy criterion at fixed intervals (Sokar et al., 2023). At each intervention point, we check all the neurons in the network using a mini-batch of training data and reset the dormant neurons as defined in Eq. (11).

C.1.4 Resetting Layer

This method involves periodically replacing the weights of the layers in the network with newly initialized values (Nikishin et al., 2022). We also provide two options for this operation: At each intervention point, the user can choose to replace the weights of the final layers or all the layers in the network.

C.2 Normlization

C.2.1 Layer Normalization

A `torch.nn.LayerNorm` function (Ba et al., 2016) is set before the activation at each layer. For convolutional layers, it is applied to the channel dimension.

C.2.2 Normalize-and-Project

The normalize-and-project (NaP) operation follows a two-step workflow: normalization and projection (Lyle et al., 2024a). For normalization, layer normalization (or RMSNorm) is inserted before every nonlinearity in the network to stabilize pre-activation statistics and enable gradient mixing, which helps revive dormant ReLU units by correlating gradients

across units. For projection, we periodically rescale the weights of each layer to their initial norms during training, decoupling parameter norm growth from the effective learning rate (ELR). This prevents ELR decay caused by unchecked norm growth while maintaining the benefits of normalization. Optionally, scale/offset parameters are either normalized jointly (for homogeneous activations) or regularized toward initial values to avoid drift. The process ensures stable training dynamics in nonstationary tasks without compromising performance on stationary benchmarks.

C.3 Regularization

C.3.1 L2 Normalization

This method (Lyle et al., 2023) adds an additional loss term to the model update, which corresponds to the L2 norm of the weights of the network. This loss is scaled by a coefficient α.

C.3.2 Regenerative Regularization

This method (Kumar et al., 2023) adds an additional loss term to the model update, which is the L2 norm of the difference between the current parameters of the network and the initial network parameters. This loss is scaled by a coefficient α.

C.3.3 Parseval Regularization

This method (Chung et al., 2024) adds an additional loss term to the model update. For each weight matrix $\mathbf{W}$, the Parseval regularization loss is defined as

$$L_{\text{Parseval}}(\mathbf{W}) = \lambda \|\mathbf{W}\mathbf{W}^{\mathrm{T}} - s\mathbf{I}\|_F, \tag{2}$$

where $\lambda > 0$ controls the regularization strength, $s > 0$ is a scaling coefficient, $\mathbf{I}$ is the identity matrix of appropriate dimension and $\|\cdot\|_F$ denotes the Frobenius norm.

C.4 Activation Function

C.4.1 CReLU Activation

This method replaces ReLU activations with the CReLU activation function (Abbas et al., 2023):

$$f(x) = \text{Concatenate}(\text{ReLU}(x), \text{ReLU}(-x)), \tag{3}$$

which ensures that the gradient is non-zero for all units in a given layer.

We concatenate the outputs of a linear layer by the feature dimension while concatenating the outputs of a convolution layer by the feature dimension.

C.4.2 Deep Fourier Features

This method (Lewandowski et al., 2025) computes deep Fourier features. It replaces standard activation functions with concatenated sine and cosine activations

$$f(x) = \text{Concatenate}(\sin(x), \cos(x)) \tag{4}$$

in every layer to dynamically balance linearity and nonlinearity for sustained plasticity in continual learning.

Similarly, we concatenate the outputs of a linear layer by the feature dimension while concatenating the outputs of a convolution layer by the feature dimension.

C.5 Optimizer

C.5.1 TRAC

TRAC (Muppidi et al., 2024) operates as a meta-algorithm layered on top of a base optimizer like gradient descent or Adam. At each time step, TRAC computes the policy gradient and uses the base optimizer to obtain a candidate update. Then, it applies a set of 1D tuners—each associated with a different discount factor—to evaluate how far to trust this candidate update versus staying near a reference point. These tuners use the Erfi potential function (Zhang et al., 2024) to dynamically adjust a scaling factor based on past gradients, and their outputs are aggregated to determine the final weight update as a convex combination of the candidate and the reference point. This online and data-dependent mechanism ensures stability and adaptability without requiring manual tuning, enabling TRAC to generalize across varied tasks and distribution shifts while mitigating both mild and extreme forms of plasticity loss.

Appendix D. Base RL Algorithms

In this paper, we select three representative RL baselines as the base algorithms, including policy-based, value-based, on-policy, and off-policy approaches.

D.1 Proximal Policy Optimization

Proximal policy optimization (PPO) (Schulman et al., 2017) is a popular on-policy algorithm for learning a continuous or discrete control policy—$\pi_{\boldsymbol{\theta}}(\boldsymbol{a}|\boldsymbol{s})$. PPO employs policy gradients using action-advantages: $A_t = A^{\pi}(\boldsymbol{a}_t, \boldsymbol{s}_t) = Q^{\pi}(\boldsymbol{a}_t, \boldsymbol{s}_t) - V^{\pi}(\boldsymbol{s}_t)$, and minimizes a clipped-ratio loss over mini-batches of recent experience (collected under $\pi_{\boldsymbol{\theta}_{\text{old}}}$):

$$L_{\pi}(\boldsymbol{\theta}) = -\mathbb{E}_{\tau\sim\pi}\left[\min\left(\rho_t(\boldsymbol{\theta})A_t, \text{clip}(\rho_t(\boldsymbol{\theta}), 1-\epsilon, 1+\epsilon)A_t\right)\right], \rho_t(\boldsymbol{\theta}) = \frac{\pi_{\boldsymbol{\theta}}(\boldsymbol{a}_t|\boldsymbol{s}_t)}{\pi_{\boldsymbol{\theta}_{\text{old}}}(\boldsymbol{a}_t|\boldsymbol{s}_t)}. \quad (5)$$

Our PPO agents learn a state-value estimator—$V_{\boldsymbol{\phi}}(\boldsymbol{s})$, which is regressed against a target of discounted returns and used with generalized advantage estimation (Schulman et al., 2015):

$$L_V(\boldsymbol{\phi}) = \mathbb{E}_{\tau\sim\pi}\left[\left(V_{\boldsymbol{\phi}}(\boldsymbol{s}_t) - V_t^{\text{target}}\right)^2\right]. \quad (6)$$

D.2 Parallel Q-Network

Parallel Q-Network (PQN) (Gallici et al., 2025) exploits parallelised sampling without a replay buffer or target networks, which is regularised with network normalization and ℓ_2 regularization. To achieve ℓ_2 regularization, it regularizes the final weight layer w through TD update vector:

$$\delta^{\text{reg}}(\phi, \varsigma) := \delta^{\text{Layer}}(\phi, \varsigma) - \left(\frac{\gamma}{2}\right)^2 \left[w^{\top} 0 \cdots 0\right]^{\top}, \quad (7)$$

where $\delta^{\text{Layer}}(\phi, \varsigma)$ is the TD update vector that adopts the LayerNorm critic—$Q_{\phi}^{\text{Layer}}(x) = w^{\top}\ \text{LayerNorm}^{\ k}[\sigma \circ Mx]$.

D.3 Twin Delayed Deep Deterministic Policy Gradient (TD3)

Twin delayed deep deterministic policy gradient (TD3) (Fujimoto et al., 2018) learns a deterministic policy $\pi_{\boldsymbol{\theta}}(\boldsymbol{s})$ and two Q-functions $Q_{\boldsymbol{\phi}_1}, Q_{\boldsymbol{\phi}_2}$ through clipped double Q-learning:

$$y_t = r_t + \gamma \min_{i=1,2} Q_{\boldsymbol{\phi}_i^-}(\boldsymbol{s}_{t+1}, \pi_{\boldsymbol{\theta}^-}(\boldsymbol{s}_{t+1}) + \epsilon), \quad (8)$$

where $\epsilon \sim \text{clip}(\mathcal{N}(0, \sigma), -c, c)$, with Q-function losses

$$L_Q(\boldsymbol{\phi}_i) = \mathbb{E}_{(\boldsymbol{s}_t, \boldsymbol{a}_t)\sim\mathcal{D}}[(Q_{\boldsymbol{\phi}_i}(\boldsymbol{s}_t, \boldsymbol{a}_t) - y_t)^2], \quad (9)$$

and policy loss

$$L_{\pi}(\boldsymbol{\theta}) = -\mathbb{E}_{\boldsymbol{s}_t\sim\mathcal{D}}[Q_{\boldsymbol{\phi}_1}(\boldsymbol{s}_t, \pi_{\boldsymbol{\theta}}(\boldsymbol{s}_t))], \quad (10)$$

employing delayed policy updates and target network stabilization.

Appendix E. Benchmark Selection

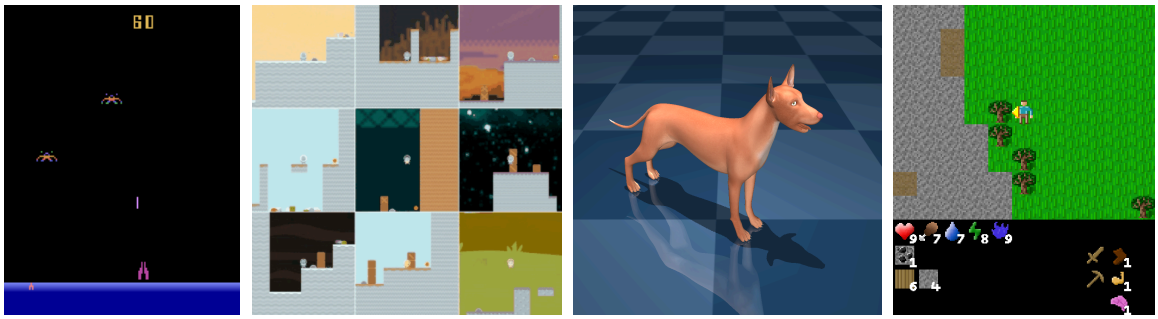

Figure 2: Screenshots of well-established ALE, Procgen, DMC, and Craftax (*left to right*).

Benchmark	Task	Observation Space	Action Space
ALE	DemonAttack	Box(0, 255, (210, 160, 3))	Discrete(6)
Procgen	StarPilot	Box(0, 255, (3, 64, 64))	Discrete(15)
DMC	Dog	Box(-inf, inf, (223,), float32)	Box(-1.0, 1.0, (38,), float32)
Craftax	Symbolic	Box(0.0, 1.0, (8268,), float32)	Discrete(43)

Table 1: Details of the challenging environments.

E.1 Standard

In the standard setting, as shown in Figure 2, we use four well-established and challenging benchmarks, *i.e.,* Arcade Learning Environment (ALE) (Bellemare et al., 2013), Procgen (Cobbe et al., 2020), and DeepMind Control Suite (DMC) (Tassa et al., 2018).

E.2 Continual

E.2.1 Variant of Procgen

For Procgen, we evaluate the adaptability of various methods using two variants: one involves increasing the level with a fixed level offset (see Figure 3(a)), while the other involves constructing a task sequence, where each sequence is a random combination of tasks (see Figure 3(b)). It is important to note that we design multiple rounds for the effective evaluation of plasticity, with the task sequence in each round being randomized.

E.2.2 Variant of DMC

To validate the effectiveness of various plasticity-based methods, we use the *Dog* as the base agent and build a task stream including five different tasks, *i.e., Stand*, *Walk*, *Trot*, *Run*, *Fetch* (see Figure 4(a)). Akin to continual Procgen (task-shift), each round is assigned a

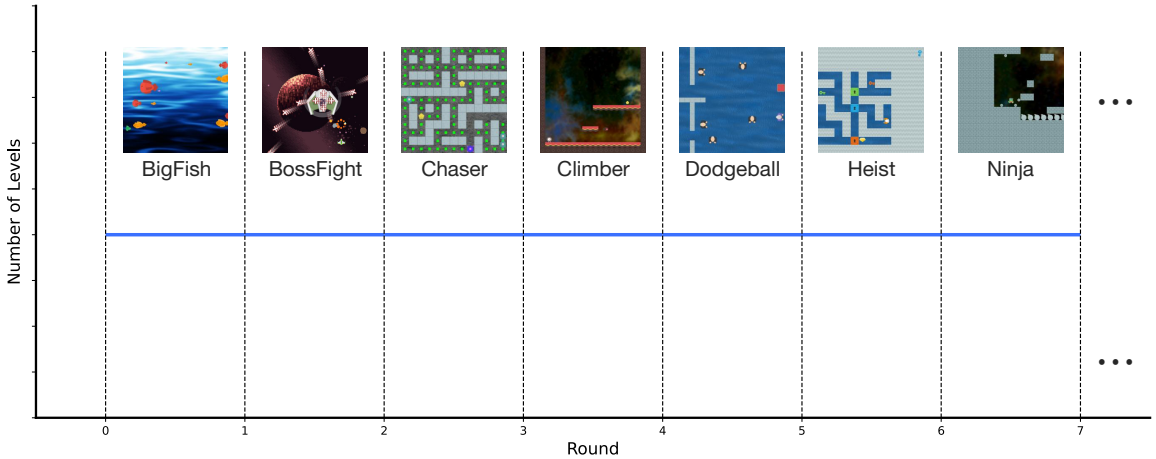

(a) Continual Procgen with cyclic task streams

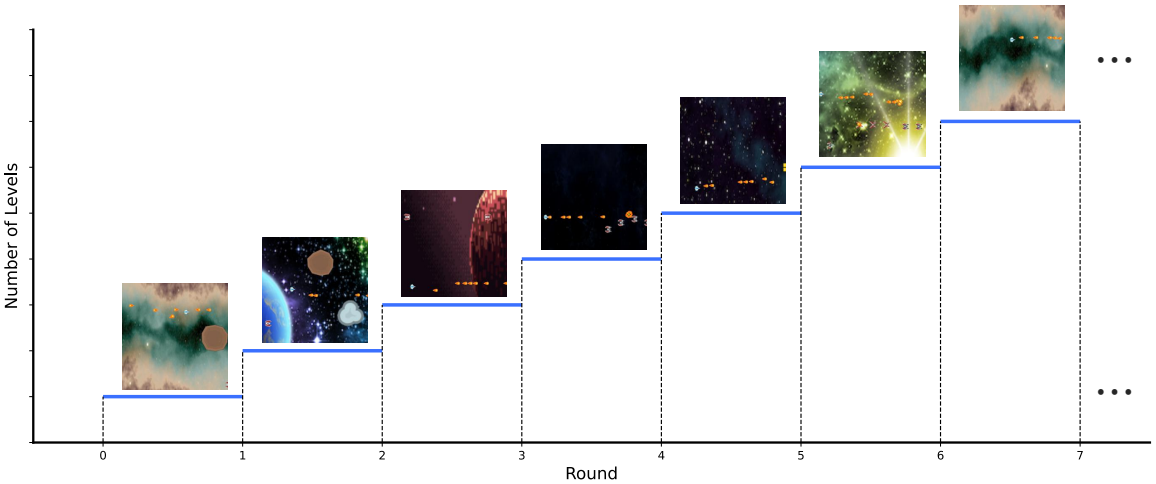

(b) Continual Procgen with level shift

Figure 3: Maintaining plasticity in continual Procgen.

random task stream. Moreover, to build a non-stationary DMC environment, as visualized in Figure 4(b), we change the dynamics of the *Quadruped* agent. Specifically, we varied the coefficient of friction by sampling it from a log-uniform distribution over the range [0.02, 2.00], applying a logarithmic scale with base 10.

E.3 Open-ended

To investigate the plasticity in an open-ended environment, we adopt Craftax (Matthews et al., 2024) as the test bunch, which evaluates the exploration and long-horizon capability of the agent.

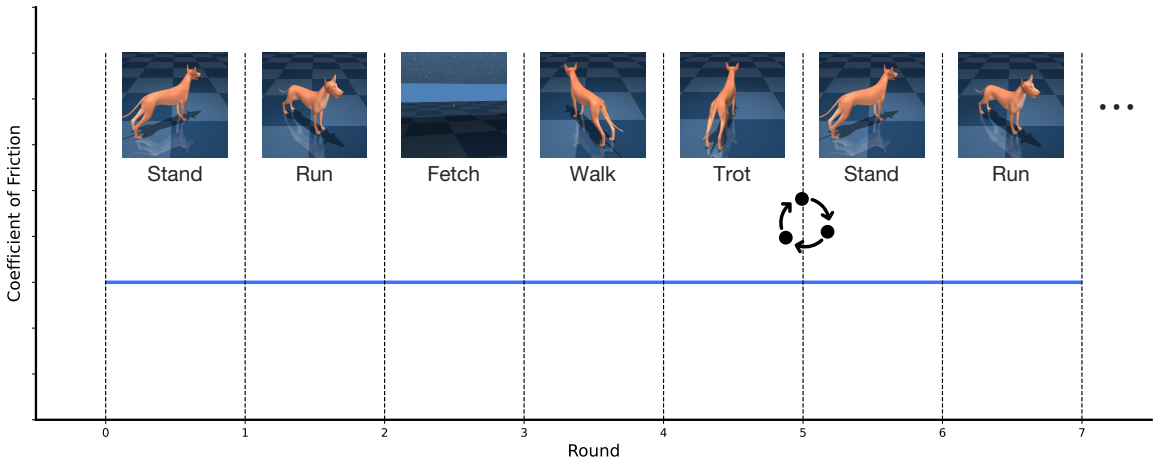

(a) Continual DMC with cyclic task streams

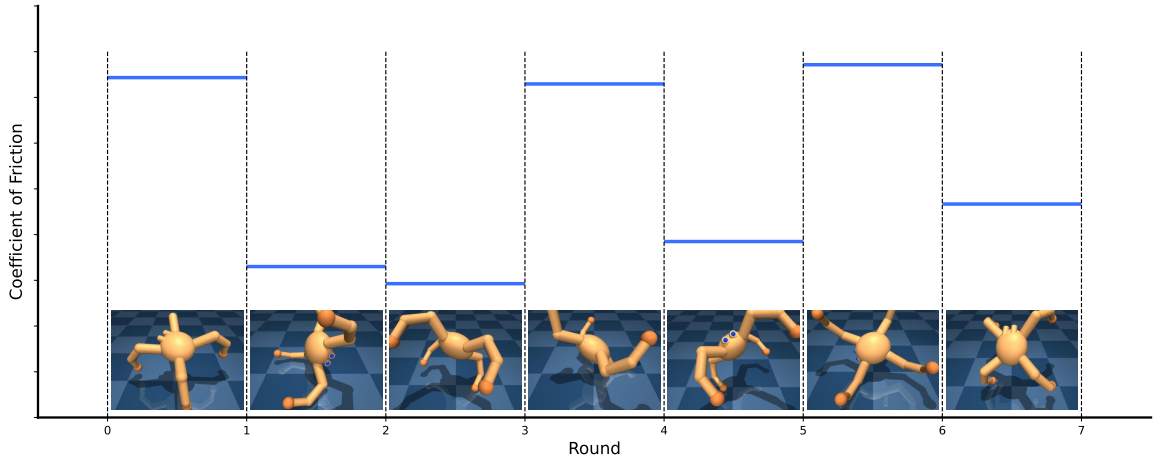

(b) Continual DMC with varying dynamic

Figure 4: Maintaining plasticity in continual DMC.

Appendix F. Plasticity-Related Evaluation Metrics

F.1 Ratio of Dormant Units

Given an input distribution $\mathcal{D}$, let $h_i^\ell(x)$ denote the activation of neuron i in layer ℓ under input $x \in \mathcal{D}$ and H^ℓ be the number of neurons in layer ℓ. We define the score of a neuron i (in layer ℓ) via the normalized average of its activation as follows (Sokar et al., 2023):

$$s_i^\ell = \frac{\mathbb{E}_{x\in\mathcal{D}}|h_i^\ell(x)|}{\frac{1}{H^\ell}\sum_{k=1}^{H^\ell}\mathbb{E}_{x\in\mathcal{D}}|h_k^\ell(x)|} \tag{11}$$

We say neuron i in layer ℓ is τ-**dormant** if $s_i^\ell \leq \tau$. Then, the ratio of dormant units (RDU) is defined as the percentage of dormant neurons among all the neurons.

F.2 Fraction of Active Units

Although the complete mechanisms underlying plasticity loss remain unclear, a reduction in the number of active units within the network has been identified as a principal factor contributing to this deterioration. Hence, the fraction of active units (FAU) is widely used as a metric for measuring plasticity. Specifically, the FAU for neurons located in module $\mathcal{M}$, is formally defined as (Ma et al., 2024):

$$\text{FAU}(\mathcal{M}) = \frac{\sum_{n\in\mathcal{M}}\mathbb{1}(a_n(x) > 0)}{N}, \tag{12}$$

where $a_n(x)$ represent the activation of neuron n given the input x, and N is the total number of neurons within module $\mathcal{M}$.

F.3 Stable Rank

The stable rank (SR) assesses the rank of the feature matrix, reflecting the diversity and richness of the representations learned by the network (Kumar et al., 2022). Denote by $\mathbf{F} \in \mathbb{R}^{n\times m}$ the feature matrix with n samples and m features, σ_k are the singular values sorted in descending order for $k = 1, \ldots, q$ and $q = \min(n, m)$, the SR is defined as

$$\text{SR}(\mathbf{F}) = \min\{k : \frac{\sum_i^k \sigma_i}{\sum_j^q \sigma_j} > 0.99\}, \tag{13}$$

F.4 Effective Rank

In the case of neural networks, the effective rank of a hidden layer measures the number of units that can produce the output of the layer (Roy and Vetterli, 2007). If a hidden layer has a low effective rank, then a small number of units can produce the output of the layer, meaning that many of the units in the hidden layer are not providing any useful information. Similar to SR, the effective rank (ER) is defined as

$$\text{ER}(\mathbf{F}) = \exp(H(p_1, \ldots, p_q)), H(p_1, \ldots, p_q) = -\sum_{k=1}^{q} p_k \log p_k, \tag{14}$$

where $q = \min(n, m)$ and $p_k = \frac{\sigma_k}{\|\boldsymbol{\sigma}\|_1}$.

F.5 Weight Magnitude

The weight magnitude is used to monitor the overall scale of the model parameters, which can provide insights into the model's capacity usage and its level of plasticity (Lyle et al., 2024b). A high weight magnitude may suggest potential overfitting or reduced adaptability due to saturation effects, while a low magnitude might indicate undertraining or high plasticity.

Formally, denote by f_Θ the neural network with a set of parameters Θ, the weight magnitude (WM) is defined as

$$\text{WM} = \sqrt{\frac{\sum_{\theta \in \Theta} \theta^2}{|\Theta|}}, \tag{15}$$

where $|\Theta|$ is the cardinality.

F.6 Weight Difference

To quantify how much a model changes during training or across different tasks in continual reinforcement learning, we compute the weight difference between two model states. This metric is useful for evaluating plasticity and adaptation, as well as detecting abrupt or minimal updates in parameter space.

Let $\boldsymbol{\theta}^{(t)} = \{\theta_1^{(t)}, \ldots, \theta_P^{(t)}\}$ denote the parameters of the model after learning task t, and $\boldsymbol{\theta}^{(t-1)}$ be the parameters before learning the task. The *L2 norm difference* between these two states is defined as (Juliani and Ash, 2024):

$$\text{WD} = \sqrt{\frac{1}{P} \sum_{p=1}^{P} \left(\theta_p^{(t)} - \theta_p^{(t-1)} \right)^2}. \tag{16}$$

This metric captures the average magnitude of change in parameters and helps assess whether the model underwent significant structural modification between training phases.

F.7 Feature Norm

The feature norm evaluates the average L2 norm of the feature vectors produced by the model, providing a quantitative measure of the feature magnitude (Kumar et al., 2022). This metric is particularly useful in continual reinforcement learning for detecting representational collapse or overly sparse activations, which may indicate reduced expressiveness or excessive regularization (Lee et al., 2024).

Given a feature matrix $\mathbf{F} \in \mathbb{R}^{n \times m}$, where n is the batch size (number of samples) and m is the dimensionality of each feature vector, the feature norm (FN) is computed as:

$$\text{FN}(\mathbf{F}) = \frac{1}{n} \sum_{i=1}^{n} \left\| \mathbf{F}_{i,:} \right\|_2, \tag{17}$$

where $\mathbf{F}_{i,:}$ denotes the i-th row of $\mathbf{F}$, corresponding to the feature representation of the i-th input.

F.8 Feature Variance

The feature variance quantifies the variability of feature activations across input samples. In continual reinforcement learning, this metric helps assess whether the model maintains diverse and informative representations over time. A collapse in feature variance may indicate overfitting, representational drift, or forgetting.

Let $\mathbf{F} \in \mathbb{R}^{n \times m}$ denote the feature matrix, where n is the number of input samples and m is the number of features. The feature variance (FV) is defined as the average variance across all feature dimensions (Lee et al., 2024):

$$\mathrm{FV}(\mathbf{F}) = \frac{1}{m} \sum_{j=1}^{m} \mathrm{Var}(\mathbf{F}_{:,j}), \tag{18}$$

where $\mathbf{F}_{:,j}$ denotes the j-th column of $\mathbf{F}$, corresponding to the j-th feature across the batch.

F.9 Gradient Norm

The gradient norm (GN) quantifies the magnitude of gradients during optimization, reflecting the learning signal's strength (Abbas et al., 2023). In continual reinforcement learning, tracking the gradient norm is essential for diagnosing issues such as vanishing gradients, overfitting, or under-training. Moreover, it provides insights into how much the model updates in response to new data or tasks.

Given a model parameter set $\boldsymbol{\theta} = \{\theta_1, \ldots, \theta_P\}$ with corresponding gradients $\nabla \mathcal{L}(\theta_p)$, the L2 norm of the gradients is defined as:

$$\mathrm{GN} = \left(\sum_{p=1}^{P} \|\nabla \mathcal{L}(\theta_p)\|_2^2 \right)^{1/2}. \tag{19}$$

F.10 Policy Entropy

Policy entropy quantifies the uncertainty or stochasticity of an agent's policy (Haarnoja et al., 2018). In reinforcement learning, higher entropy encourages exploration by promoting diverse actions, while lower entropy indicates more deterministic (exploitative) behavior. In continual reinforcement learning, monitoring policy entropy helps analyze whether the agent becomes overconfident (risking forgetting) or maintains sufficient exploration across tasks.

Let $\pi(\boldsymbol{a}|\boldsymbol{s})$ denote the probability of selecting action $\boldsymbol{a}$ under state $\boldsymbol{s}$ according to the policy π. The entropy of the policy at a given state is defined as:

$$H(\pi(\cdot|\boldsymbol{s})) = -\sum_{\boldsymbol{a} \in \mathcal{A}} \pi(\boldsymbol{a}|\boldsymbol{s}) \log \pi(\boldsymbol{a}|\boldsymbol{s}), \tag{20}$$

where $\mathcal{A}$ is the set of possible actions. Given a batch of states $\{\boldsymbol{s}_1, \ldots, \boldsymbol{s}_n\}$, the average policy entropy (PE) is:

$$\mathrm{PE} = \frac{1}{n} \sum_{i=1}^{n} H(\pi(\cdot|\boldsymbol{s}_i)). \tag{21}$$

Appendix G. Experiments

Working in progress...

G.1 Standard RL Scenario

G.1.1 PPO+Procgen

Table 2: Default hyperparameters used for the PPO+Procgen experiments.

Hyperparameter	Value	Hyperparameter	Value
Observation downsampling	(64, 64)	Optimizer	Adam
Observation normalization	/ 255.	Learning rate	5e-4
Reward normalization	No	GAE coefficient	0.95
Weight initialization	Orthogonal	Action entropy coefficient	0.01
LSTM	No	Value loss coefficient	0.5
Stacked frames	No	Value clip range	0.2
Environment steps	25000000	Max gradient norm	0.5
Episode steps	256	Epochs per rollout	3
Number of workers	1	Batch size	2048
Environments per worker	64	Discount factor	0.999

G.1.2 PQN+ALE

Table 3: Default hyperparameters used for the PQN+ALE experiments.

Hyperparameter	Value	Hyperparameter	Value
Observation downsampling	(84, 84)	Starting epsilon for exploration	1
Observation normalization	/ 255.	Ending epsilon for exploration	0.01
Reward normalization	No	Fraction of exploration	0.1
Weight initialization	Orthogonal	Lambda for Q-learning	0.65
LSTM	No	GAE coefficient	0.95
Stacked frames	4	Action entropy coefficient	0.01
Environment steps	10000000	Value loss coefficient	0.5
Episode steps	128	Value clip range	0.2
Number of workers	1	Max gradient norm	10.0
Environments per worker	8	Epochs per rollout	4
Optimizer	Adam	Batch size	256
Learning rate	2.5e-4	Discount factor	0.99

Table 4: Default hyperparameters used for the TD3+DMC experiments.

Hyperparameter	**Value**	**Hyperparameter**	**Value**
Warm-up steps	1e4	Environments per worker	1
Replay buffer size	1e6	Optimizer	Adam
State normalization	No	Learning rate	1e-4
Reward normalization	No	Target smoothing coefficient	0.005
Weight initialization	Orthogonal	Target policy noise	0.2
LSTM	No	Target noise clip	0.5
Non-linearity	ReLU	Policy delay	2
Environment steps	5e6	Batch size	256
Number of workers	1	Discount factor	0.99

G.1.3 TD3+DMC

G.2 Continual RL Scenario

G.3 Open-ended RL Scenario

Table 5: Default hyperparameters used for the PPO+Craftax experiments.

Hyperparameter	**Value**	**Hyperparameter**	**Value**
Observation downsampling	N/A	Optimizer	Adam
Observation normalization	None	Learning rate	2e-4
Reward normalization	No	GAE coefficient	0.8
Weight initialization	Orthogonal	Action entropy coefficient	0.01
LSTM	No	Value loss coefficient	0.5
Stacked frames	N/A	Value clip range	0.2
Environment steps	100M	Max gradient norm	1.0
Episode steps	64	Epochs per rollout	4
Number of workers	1	Batch size	8192
Environments per worker	1024	Discount factor	0.99

Appendix H. Author Contributions

We summarize the main contributions from each author as follows (names are listed in alphabetical order):

- **Project Lead**: Mingqi Yuan
- **Algorithm Development**: Mingqi Yuan
- **Environment Development**: Qi Wang
- **Metric Development and Project Evaluation**: Guozheng Ma
- **Area Advisor**: Bo Li, Tao Yu, Xin Jin, and Yunbo Wang
- **Supervision**: Dacheng Tao, Wenjun Zeng, and Xiaokang Yang

References

Z. Abbas, R. Zhao, J. Modayil, A. White, and M. C. Machado. Loss of plasticity in continual deep reinforcement learning. In *Conference on Lifelong Learning Agents*, pages 620–636. PMLR, 2023.

D. Abel, A. Barreto, B. Van Roy, D. Precup, H. P. van Hasselt, and S. Singh. A definition of continual reinforcement learning. *Advances in Neural Information Processing Systems*, 36:50377–50407, 2023.

J. Ash and R. P. Adams. On warm-starting neural network training. *Advances in neural information processing systems*, 33:3884–3894, 2020.

J. L. Ba, J. R. Kiros, and G. E. Hinton. Layer normalization. In *NIPS 2016 Deep Learning Symposium*, 2016.

M. G. Bellemare, Y. Naddaf, J. Veness, and M. Bowling. The arcade learning environment: An evaluation platform for general agents. *Journal of artificial intelligence research*, 47: 253–279, 2013.

J. S. O. Ceron, M. G. Bellemare, and P. S. Castro. Small batch deep reinforcement learning. In *Thirty-seventh Conference on Neural Information Processing Systems*, 2023. URL `https://openreview.net/forum?id=wPqEvmwFEh`.

W. Chung, L. Cherif, D. Precup, and D. Meger. Parseval regularization for continual reinforcement learning. *Advances in Neural Information Processing Systems*, 37:127937–127967, 2024.

K. Cobbe, C. Hesse, J. Hilton, and J. Schulman. Leveraging procedural generation to benchmark reinforcement learning. In *International conference on machine learning*, pages 2048–2056. PMLR, 2020.

S. Dohare, J. F. Hernandez-Garcia, Q. Lan, P. Rahman, A. R. Mahmood, and R. S. Sutton. Loss of plasticity in deep continual learning. *Nature*, 632(8026):768–774, 2024.

S. Fujimoto, H. Hoof, and D. Meger. Addressing function approximation error in actor-critic methods. In *International conference on machine learning*, pages 1587–1596. PMLR, 2018.

A. Galashov, M. Titsias, A. György, C. Lyle, R. Pascanu, Y. W. Teh, and M. Sahani. Non-stationary learning of neural networks with automatic soft parameter reset. *Advances in Neural Information Processing Systems*, 37:83197–83234, 2024.

M. Gallici, M. Fellows, B. Ellis, B. Pou, I. Masmitja, J. N. Foerster, and M. Martin. Simplifying deep temporal difference learning. In *ICLR*, 2025.

T. Haarnoja, A. Zhou, P. Abbeel, and S. Levine. Soft actor-critic: Off-policy maximum entropy deep reinforcement learning with a stochastic actor. In *International conference on machine learning*, pages 1861–1870. PMLR, 2018.

S. Huang, R. F. J. Dossa, C. Ye, J. Braga, D. Chakraborty, K. Mehta, and J. G. Araújo. Cleanrl: High-quality single-file implementations of deep reinforcement learning algorithms. *Journal of Machine Learning Research*, 23(274):1–18, 2022. URL `http://jmlr.org/papers/v23/21-1342.html`.

A. Juliani and J. Ash. A study of plasticity loss in on-policy deep reinforcement learning. *Advances in Neural Information Processing Systems*, 37:113884–113910, 2024.

T. Klein, L. Miklautz, K. Sidak, C. Plant, and S. Tschiatschek. Plasticity loss in deep reinforcement learning: A survey. *arXiv preprint arXiv:2411.04832*, 2024.

A. Kumar, R. Agarwal, T. Ma, A. Courville, G. Tucker, and S. Levine. DR3: Value-based deep reinforcement learning requires explicit regularization. In *International Conference on Learning Representations*, 2022. URL `https://openreview.net/forum?id=POvMvLi91f`.

S. Kumar, H. Marklund, and B. Van Roy. Maintaining plasticity in continual learning via regenerative regularization. *arXiv preprint arXiv:2308.11958*, 2023.

H. Lee, H. Cho, H. Kim, D. Gwak, J. Kim, J. Choo, S.-Y. Yun, and C. Yun. Plastic: Improving input and label plasticity for sample efficient reinforcement learning. *Advances in Neural Information Processing Systems*, 36:62270–62295, 2023.

H. Lee, D. Hwang, D. Kim, H. Kim, J. J. Tai, K. Subramanian, P. R. Wurman, J. Choo, P. Stone, and T. Seno. Simba: Simplicity bias for scaling up parameters in deep reinforcement learning. *arXiv preprint arXiv:2410.09754*, 2024.

H. Lee, Y. Lee, T. Seno, D. Kim, P. Stone, and J. Choo. Hyperspherical normalization for scalable deep reinforcement learning. *arXiv preprint arXiv:2502.15280*, 2025.

A. Lewandowski, D. Schuurmans, and M. C. Machado. Plastic learning with deep fourier features. In *The Thirteenth International Conference on Learning Representations*, 2025. URL `https://openreview.net/forum?id=NIkfix2eDQ`.

C. Lyle and R. Pascanu. Switching between tasks can cause ai to lose the ability to learn, 2024.

C. Lyle, M. Rowland, and W. Dabney. Understanding and preventing capacity loss in reinforcement learning. *arXiv preprint arXiv:2204.09560*, 2022.

C. Lyle, Z. Zheng, E. Nikishin, B. A. Pires, R. Pascanu, and W. Dabney. Understanding plasticity in neural networks. In *International Conference on Machine Learning*, pages 23190–23211. PMLR, 2023.

C. Lyle, Z. Zheng, K. Khetarpal, J. Martens, H. P. van Hasselt, R. Pascanu, and W. Dabney. Normalization and effective learning rates in reinforcement learning. *Advances in Neural Information Processing Systems*, 37:106440–106473, 2024a.

C. Lyle, Z. Zheng, K. Khetarpal, H. van Hasselt, R. Pascanu, J. Martens, and W. Dabney. Disentangling the causes of plasticity loss in neural networks. *arXiv preprint arXiv:2402.18762*, 2024b.

G. Ma, L. Li, S. Zhang, Z. Liu, Z. Wang, Y. Chen, L. Shen, X. Wang, and D. Tao. Revisiting plasticity in visual reinforcement learning: Data, modules and training stages. In *The Twelfth International Conference on Learning Representations*, 2024. URL `https://openreview.net/forum?id=0aR1s9YxoL`.

M. Matthews, M. Beukman, B. Ellis, M. Samvelyan, M. Jackson, S. Coward, and J. Foerster. Craftax: A lightning-fast benchmark for open-ended reinforcement learning. In *ICML*, 2024.

A. Muppidi, Z. Zhang, and H. Yang. Fast trac: A parameter-free optimizer for lifelong reinforcement learning. *Advances in Neural Information Processing Systems*, 37:51169–51195, 2024.

M. Nauman, M. Ostaszewski, K. Jankowski, P. Miłoś, and M. Cygan. Bigger, regularized, optimistic: scaling for compute and sample-efficient continuous control. In *Advances in Neural Information Processing Systems*, 2024.

E. Nikishin. *Parameter, experience, and compute efficient deep reinforcement learning*. PhD thesis, Université de Montréal, 2024.

E. Nikishin, M. Schwarzer, P. D'Oro, P.-L. Bacon, and A. Courville. The primacy bias in deep reinforcement learning. In *International conference on machine learning*, pages 16828–16847. PMLR, 2022.

E. Nikishin, J. Oh, G. Ostrovski, C. Lyle, R. Pascanu, W. Dabney, and A. Barreto. Deep reinforcement learning with plasticity injection. *Advances in Neural Information Processing Systems*, 36:37142–37159, 2023.

S. Park, I. Han, S. Oh, and K.-J. Kim. Activation by interval-wise dropout: A simple way to prevent neural networks from plasticity loss. *arXiv preprint arXiv:2502.01342*, 2025.

O. Roy and M. Vetterli. The effective rank: A measure of effective dimensionality. In *2007 15th European signal processing conference*, pages 606–610. IEEE, 2007.

J. Schulman, P. Moritz, S. Levine, M. Jordan, and P. Abbeel. High-dimensional continuous control using generalized advantage estimation. *Proceedings of the International Conference on Learning Representations*, 2015.

J. Schulman, F. Wolski, P. Dhariwal, A. Radford, and O. Klimov. Proximal policy optimization algorithms. *arXiv preprint arXiv:1707.06347*, 2017.

D. Silver and R. S. Sutton. Welcome to the era of experience, 2025. URL `https://storage.googleapis.com/deepmind-media/Era-of-Experience%20/The%20Era%20of%20Experience%20Paper.pdf`. Preprint of a chapter to appear in the book "Designing an Intelligence", published by MIT Press.

G. Sokar, R. Agarwal, P. S. Castro, and U. Evci. The dormant neuron phenomenon in deep reinforcement learning. In *International Conference on Machine Learning*, pages 32145–32168. PMLR, 2023.

D. Tarasov, A. Nikulin, D. Akimov, V. Kurenkov, and S. Kolesnikov. Corl: Research-oriented deep offline reinforcement learning library. *Advances in Neural Information Processing Systems*, 36:30997–31020, 2023.

Y. Tassa, Y. Doron, A. Muldal, T. Erez, Y. Li, D. d. L. Casas, D. Budden, A. Abdolmaleki, J. Merel, A. Lefrancq, et al. Deepmind control suite. *arXiv preprint arXiv:1801.00690*, 2018.

Z. Zhang, D. Bombara, and H. Yang. Discounted adaptive online learning: Towards better regularization. In *International Conference on Machine Learning*, pages 58631–58661. PMLR, 2024.